Real-time Point of Interest Segmentation for Electron Microscopy Images via Machine Learning

Michael Lin[1], Yousra Nahas[2], Prokhorenko Sergei[2], Sujit Das[3], Ruijuan Xu[4], Harold Y. Hwang[5], Ramamoorthy Ramesh[6], Laurent Bellaiche[2], David A. Muller[7], Yu-Tsun Shao[8], Donglai Wei[1]

[1] Computer Science Department, Boston College – Chestnut Hill, MA, United States.
[2] Physics Department and Institute for Nanoscience and Engineering, University of Arkansas – Fayetteville, AR, United States.
[3] Materials Research Centre, Indian Institute of Science, Bangalore – Bangalore, India.
[4] Department of Materials Science and Engineering, North Carolina State University, Raleigh, NC, USA.
[5] Department of Applied Physics, Stanford University, Stanford, CA, USA.
[6] Department of Materials Science and Nanoengineering, Rice University, Houston, TX, USA.
[7] School of Applied and Engineering Physics, Cornell University, Ithaca, New York, USA.
[8] Mork Family Department of Chemical Engineering and Materials Science, University of Southern California – Los Angeles, CA, United States.

Manual segmentation of points of interests in scanning transmission electron microscopy (EM) images is difficult due to the difficulty of noise estimation and, importantly, the high temporal cost of labor. Leveraging deep learning models significantly decreases the requisite amount of manual labeling while providing a solution with workable levels of accuracy. Here, we implement the U-Net model [1] on a small sub-sequence of 17 STEM images to accelerate the labeling process for a recorded video of 81 frames with a focal interest in model performance under limited data scenarios (Figure 1).

Here, the time series STEM images are acquired on a lifted-off, ferroelectric perovskite $(SrTiO_3)/(PbTiO_3)/(SrTiO_3)$ heterostructure, which exhibit labyrinth domain patterns consisting of polar merons (end-points) and anti-merons (tri-junctions) as shown in Figure 2. The nm-sized merons and anti-merons consist of swirling electric dipoles that would minimize the bound charge and remain charge neutral for the whole system. When a focused electron probe is introduced, the electric field gradients around the probe would cause corresponding changes in the structure of (anti-)merons and their transformations, inducing topological phase transitions.

The automated segmentation of these merons and antimerons is accomplished through the training of two similar U-Net models, one of which detects merons and the other, antimerons. Raw images from the EM equipment are preprocessed through a 5%-95% clipping of intensity values, followed by normalization and application of a median blur filter for naive noise correction. Points of interest are highlighted using an annotation tool with points of interest represented as peaks in a Gaussian heatmap. The image and masks are reshaped into a single-channel image of shape 1995 pixels by 1995 pixels. The appropriate U-Net model is trained on sets of images and mask utilizing randomly applied rotations and reflections to artificially increase dataset size. The model is trained on a subset of 17 images from the sequence and validated on the final image over 10000 epochs.

Results show high levels of precision and recall (~0.7 for both) for meron detection when evaluated on the entire sequence. False positive rates and false negative rates on the entire sequence is correspondingly promising at 2.9% and 3.3%, respectively. Results for antimeron detection are more mixed, with low levels of false positive detections (2.7%) but high levels of false negatives (28%). Model inference takes 0.027 seconds per instance, enabling real-time segmentation of STEM images taken at 5-second intervals. [2]

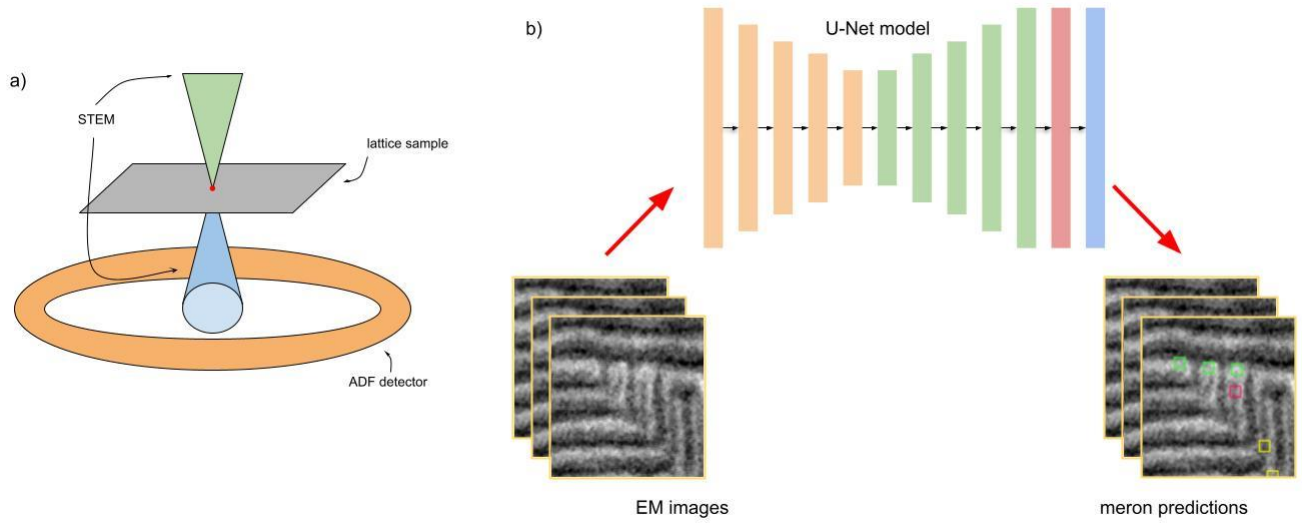

Figure 1: a) STEM setup for EM image capture. b) Pipeline for meron predictions utilizing the U-Net model for inference.

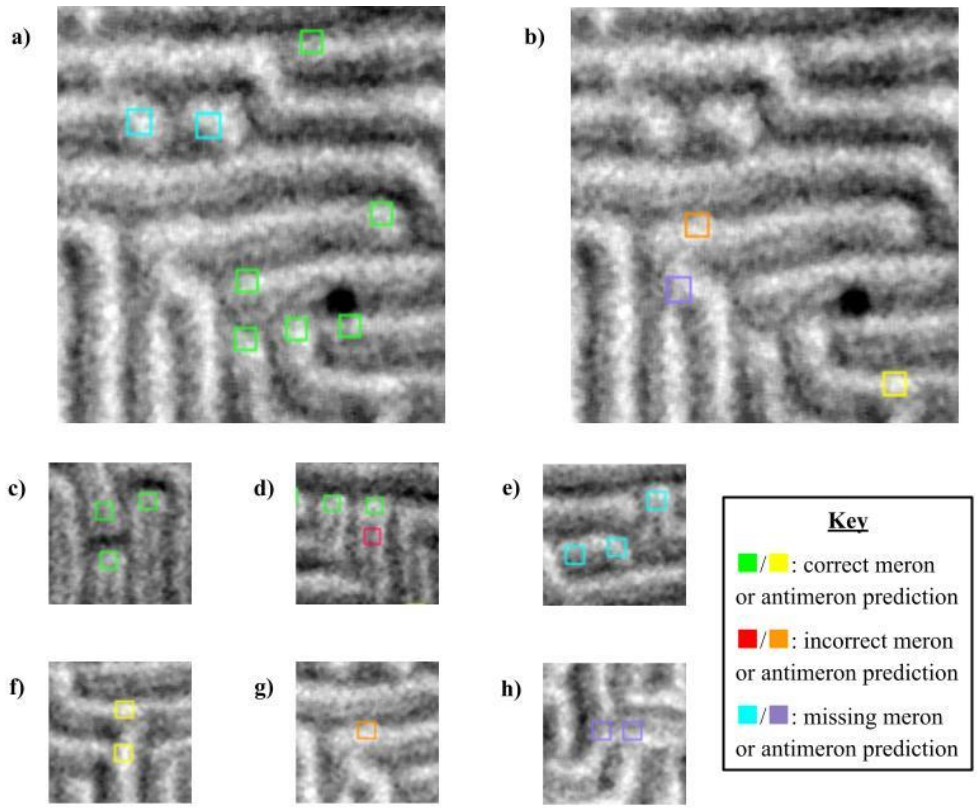

Figure 2: Method performance on a portion of a randomly selected slide. Note the lack of incorrect predictions but noticeable frequency of missing detections. a) Meron prediction results. b) Antimeron prediction results. c) Correct meron predictions. d) An incorrect meron prediction. e) Missing/undetected merons. f) Correct antimeron predictions. g) An incorrect antimeron prediction. h) Missing/undetected antimerons.

References

[1] Ronneberger *et al.*, arXiv:1505.04597 (2015).
[2] Work supported by the AFOSR Hybrid Materials MURI, award # FA9550-18-1-0480. Facilities supported by the National Science Foundation (DMR-1429155, DMR-2039380, DMR-1719875). Work partially supported by the startup funding at USC Viterbi and the USC Research and Innovation Instrumentation Award.